

Temperature as an external field for colloid–polymer mixtures: ‘quenching’ by heating and ‘melting’ by cooling

This article has been downloaded from IOPscience. Please scroll down to see the full text article.

2012 J. Phys.: Condens. Matter 24 464128

(<http://iopscience.iop.org/0953-8984/24/46/464128>)

View [the table of contents for this issue](#), or go to the [journal homepage](#) for more

Download details:

IP Address: 114.150.39.28

The article was downloaded on 16/11/2012 at 15:09

Please note that [terms and conditions apply](#).

Temperature as an external field for colloid–polymer mixtures: ‘quenching’ by heating and ‘melting’ by cooling

Shelley L Taylor¹, Robert Evans² and C Patrick Royall¹

¹ School of Chemistry, University of Bristol, Bristol, BS8 1TS, UK

² H H Wills Physics Laboratory, University of Bristol, Bristol, BS8 1TL, UK

E-mail: paddy.royall@bristol.ac.uk

Received 1 May 2012, in final form 1 August 2012

Published 31 October 2012

Online at stacks.iop.org/JPhysCM/24/464128

Abstract

We investigate the response to temperature of a well-known colloid–polymer mixture. At room temperature the gas–liquid critical value of the second virial coefficient of the effective pairwise colloid–colloid interaction for the Asakura–Oosawa model predicts the onset of gelation observed experimentally with remarkable accuracy. Upon cooling the system the effective attraction between colloids induced by polymer depletion is reduced, because the polymer radius of gyration decreases as the θ -temperature is approached. Paradoxically this raises the effective temperature, leading to ‘melting’ of colloidal gels. We find that the Asakura–Oosawa model of effective colloid interactions, together with a simple description of the polymer temperature response, provides a quantitative description of the observed location of the fluid–gel transition in the colloid volume fraction polymer reservoir number density plane. Further, we present evidence for enhancement of crystallization rates in the vicinity of the metastable critical point.

(Some figures may appear in colour only in the online journal)

1. Introduction

Colloid–polymer mixtures occupy a special place in soft matter physics [1, 2]. The introduction of non-adsorbing polymer introduces an effective attraction between the colloids whose strength and range can be tuned by altering the concentration and molecular weight, respectively, of the polymer [2–6]. The existence of this entropy driven depletion attraction opens up a vast swathe of behaviour inaccessible to colloidal systems with purely repulsive interactions, such that colloid–polymer mixtures may be regarded as true ‘model atomic systems’ [1]. The best known examples include liquid–gas phase separation [1, 2] but there are also phenomena not seen in atomic systems such as gelation [1] and re-entrant glassy dynamics at high density [7]. Real-space analysis at the particle level has enabled direct observation of local phenomena common to most condensed matter systems such as crystallization [8], and behaviour related to liquid–gas phase separation such as capillary wave fluctuations at

(colloidal) liquid–gas interfaces [9] and some properties of critical scaling [10]. Moreover colloid–polymer mixtures with a relatively short-ranged attractive interaction can (crudely) model proteins and may exhibit two-step crystal nucleation phenomena [11], to which we return below.

Theoretical treatments of colloid–polymer mixtures are based largely on the Asakura–Oosawa–Vrij (AO) model [3, 4, 6] which treats the colloid–colloid interaction as that of hard-spheres (HS) and the polymer–polymer interaction as ideal, i.e. the polymer coils are assumed to be perfectly interpenetrating spheres. However, the polymer spheres have an excluded volume (hard) interaction with the HS colloids. This model binary (AO) mixture provides the simplest, zeroth-order description of the real mixture. It is characterized by the size ratio $q = \sigma_p/\sigma$, where σ is the colloid diameter and σ_p is the polymer sphere diameter. The colloid–polymer interaction is infinite for separations $r < (\sigma + \sigma_p)/2$. From simulation and theoretical studies it is well-known that for sufficiently large size ratios, $q \gtrsim 0.3$, the AO model exhibits

fluid–fluid phase separation into a colloid-rich (liquid) and a colloid-poor (gas) phase at sufficiently high polymer volume fractions. For smaller size ratios this phase transition becomes metastable w.r.t. the fluid–crystal transition [12–14]. The same trend in phase behaviour (with σ_p set equal to twice the radius of gyration of the non-adsorbing polymer) is found in experimental studies [1, 2, 15]. In addition to predicting purely entropy driven fluid–fluid phase separation the AO model exhibits the elegant feature that for size ratios $q < (2/\sqrt{3} - 1) = 0.1547$ the degrees of freedom of the ideal polymer can be integrated out exactly and the binary mixture maps formally to a one-component system of colloids described by an effective Hamiltonian containing only one and two-body (pair) contributions [12, 14]. The former contribution plays no role in determining phase equilibrium or structure, for a uniform (bulk) fluid, but does determine the total pressure and compressibility [16]. The effective pair interaction between the colloids, given by integrating out the ideal polymer, is the standard AO potential:

$$\beta u_{AO}(r) = \begin{cases} \infty & \text{for } r < \sigma \\ -\phi_p \frac{(1+q)^3}{q^3} \left[1 - \frac{3r}{2(1+q)\sigma} + \frac{r^3}{2(1+q)^3\sigma^3} \right] & \text{for } \sigma < r < \sigma + \sigma_p \\ 0 & \text{for } r < \sigma + \sigma_p. \end{cases} \quad (1)$$

β is $1/k_B T$ where k_B is Boltzmann’s constant and T is temperature. Since the analysis is performed in the semi-grand ensemble the polymer volume fraction in the reservoir $\phi_p = \pi\sigma_p^3 z_p/6$ appears in equation (1). The polymer fugacity z_p is equal to the number density ρ_p of ideal polymers in the reservoir at the given chemical potential μ_p . As noted already, in relating the AO model to experiment, one usually sets $\sigma_p = 2R_G$ where R_G is the polymer radius of gyration. Hitherto, most work on colloidal–polymer mixtures was carried out at a fixed temperature, typically around 25 °C. Effective temperature is varied by changing the interaction strength. The effective temperature is inversely proportional to the depth of the attractive well of the interaction potential in equation (1), and is therefore fixed for a given polymer reservoir density. Scanning a phase diagram then requires preparation of a considerable number of different samples. Conversely, in molecular systems, since interactions are usually constant over the (broad) temperature range of interest, one sample is prepared and temperature is used as a control parameter.

In our present experimental study we note that colloid–polymer mixtures can respond to temperature in an intriguing and counter-intuitive manner. The effective temperature in equation (1) is set by z_p which in turn is equal to the polymer number density for ideal polymers. Real systems approximate this behaviour very well [17]. Thus the primary response of the system to temperature is given by the response of the polymer depletant, since the polymer–polymer interactions are weak and direct colloid–colloid interactions

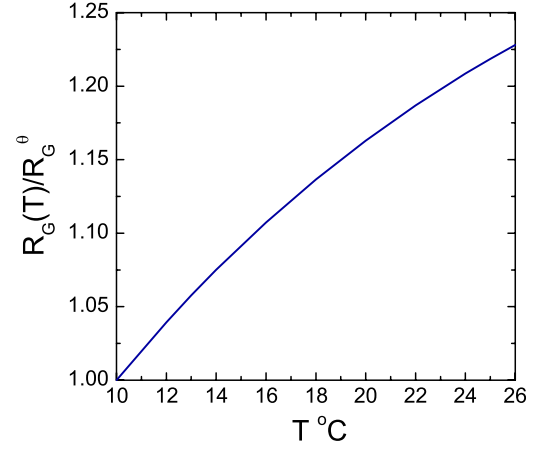


Figure 1. The radius of gyration R_G of polystyrene. This is a fit, equation (2), to experimental data [31].

are athermal (hard sphere). Now, close to (but above) their theta temperature T^θ , polymers expand (R_G increases) upon heating (figure 1). This expansion reflects the crossover, as a function of temperature, from θ -conditions where $R_G \sim N^{1/2}$, to ‘good-solvent’ conditions at higher temperature where $R_G \sim N^{3/5}$. Here N is the number of monomers in the chain [18]. This expansion has two effects: firstly, the polymer–colloid size ratio q increases, thereby increasing the range of attraction, and secondly, the polymer reservoir volume fraction $\phi_p = \pi\rho_p\sigma_p^3/6$ also increases. Since the well-depth $-\beta u_{AO}(\sigma) = \pi\rho_p\sigma^3 q^2(1 + \frac{2}{3}q)/4$ this means the effective temperature falls strongly for a modest increase in polymer size which leads to a paradoxical result, namely raising the temperature of a colloid–polymer mixture near T^θ brings about a strong effective cooling. Although this effect has been exploited to drive phase transitions in mixtures of colloidal rods and polymers [19], these temperature-dependent depletion interactions have received relatively little attention. This is in contrast to other means of controlling the attractive interactions between colloids *in situ*, such as the critical Casimir effect [20–22] and multiaxial electric fields [23]. We note that *in situ* control of attractive interactions, combined with particle-resolved studies, has the power to provide much new insight into a variety of phenomena, including phase transitions [24].

Here we make a quantitative experimental investigation, at the single-particle level, of the effect of temperature on an already well-studied colloid–polymer mixture. The elucidation of our results requires theoretical underpinning and we shall base this on the AO model described above. Specifically we investigate a mixture where the size ratio is about 0.2 but varies by 10% or so on changing temperature. The size ratio is such that the fluid–fluid (colloidal gas–liquid) transition is metastable w.r.t. the fluid–crystal transition and therefore we consider out-of-equilibrium phenomena associated with metastable states. That is to say, the equilibrium condition is colloidal gas–crystal coexistence. However, over our observation times crystallization is only obtained close to criticality, and therefore the usual liquid–gas coexistence and critical phenomena can be observed, despite

the fact that the system is metastable. A recent simulation study [25] provides a helpful framework for placing our results in context. These authors study the effective one-component AO model, where the pair potential is given by equation (1), for $q = 0.15$ which is in the regime where the mapping to the effective one-component description using only a pair potential is exact. By changing the polymer reservoir density, equivalent to changing the depth of the attractive potential well, they determine both equilibrium and out-of-equilibrium phase behaviour. More specifically, using Monte Carlo and Brownian dynamics, they investigate crystal nucleation and the onset of gelation in the vicinity of the metastable gas–liquid binodal. They present convincing evidence that crystallization is enhanced in the vicinity of the binodal. We tackle the same issues in our experiments on a real colloid–polymer mixture, seeking to ascertain what role proximity to the binodal plays in forming gels and in determining crystal nucleation rates.

It is well-known that in experiments equilibrium is often not reached and in particular gelation can occur. This phenomenon has been linked to spinodal decomposition associated with (metastable) colloidal gas–liquid condensation [26, 27]; gels are supposed to form within the accompanying fluid–fluid spinodal. It follows that knowledge of the (metastable) critical point is important in predicting where gelation might occur [27].

The connection between critical density fluctuations and crystal nucleation rates in systems with short-ranged attractive interactions, where the gas–liquid critical point is metastable with respect to crystallization, has received considerable attention since it was elucidated by Ten Wolde and Frenkel [28]. Critical fluctuations are expected to enhance the nucleation rate and may be responsible for the strong temperature dependence of nucleation rates found in globular proteins [29, 30]. In these studies a two-step nucleation process is envisaged where nuclei preferentially form in fluctuations of high density since the surface tension between the nucleus and the surrounding fluid is smaller. The reduction in free energy barrier to nucleation associated with such density fluctuations has been measured in a quasi-two dimensional depletion system [11]. Here we investigate crystallization in the neighbourhood of the metastable critical point.

This paper is organized as follows. In section 2 we first introduce the experimental system, and discuss the response of the polymer component to temperature. We then describe relating experiment and theory in terms of the AO model. In section 3 we present results for (i) the room-temperature phase diagram, (ii) crystallization around the metastable critical point and (iii) the response of the system to temperature. We conclude in section 4.

2. Methods

2.1. Experimental details

Our experimental system is based on polymethyl methacrylate (PMMA) colloids. The colloid diameter $\sigma = 1080$ nm

with polydispersity 4.6%, as determined from static light scattering. The polystyrene polymer used has a molecular weight $M_w = 8.5 \times 10^6$, which corresponds to a radius of gyration of $R_G^\theta = 95$ nm under θ conditions [32]. This leads to a polymer–colloid size ratio of $q(T = T^\theta) = 0.176$. The colloids and polymer are dispersed in *cis* decalin, where we find T^θ of polystyrene is 10 °C. We image this system at the single-particle level with a Leica SP5 confocal microscope. To this microscope we have fitted a temperature stage which uses a Peltier chip to cool from room temperature (25 °C) to the θ -temperature and below. Note that our experimental system is not density-matched. The gravitational length $\lambda_g = k_B T / (mg) = 1.96\sigma$, where m is the buoyant mass of the colloid and g is the acceleration due to gravity. Sedimentation therefore becomes an issue at long times, limiting our experimental timescales to about 1 h.

For studies of crystallization, we adopt a slightly different approach. Here we orient the sample capillaries perpendicular to gravity. Since the length of the capillary (5 cm) is very much greater than the depth (100 μ m), the effects of gravity in this orientation are minimal. The samples remain in the vertical orientation for up to 6 days. Prior to imaging, samples are carefully rotated back to the usual horizontal orientation. We note that for this system a disordered layer forms on the capillary walls which inhibits heterogeneous nucleation.

The effect of temperature on the radius of gyration of the polymer is shown in figure 1. We plot the following expression

$$R_G(T) = R_G^\theta \left[\sqrt{2} \left(1 - \exp\left(\frac{T^\theta - T}{\tau}\right) \right) + 1 \right] \quad (2)$$

for $T \geq T^\theta$ which matches closely experimental data [31] over the relevant temperature range. Here the parameter $\tau = 20$ °C.

2.2. Comparison with theory

As mentioned in section 1 we choose to interpret our experimental results within the framework of the simple AO model. A key ingredient is locating, in the AO phase diagram, the (metastable) gas–liquid binodal for size ratios $q \sim 0.2$. There are computer simulation results for the binodal and its critical point for $q = 0.1$ [14, 33] and for $q = 0.15$ [25]. Clearly in both cases $q < 0.1547$ so the mapping to an effective one-component fluid described by only the pair potential equation (1) is exact. Although our experimental systems have $q \sim 0.2$, within the context of AO we can expect three-body contributions to the effective Hamiltonian to play only a very small role. In order to ascertain the phase behaviour of the AO model it is tempting to turn to the free-volume theory [13, 14] which yields simple recipes for calculating both fluid–solid and colloidal gas–liquid phase equilibria for the binary AO mixture. This approximation is fairly successful for size ratios $\gtrsim 0.4$ [34, 35]. However, for $q = 0.1$ free-volume theory provides a reasonably accurate description of fluid–solid coexistence [14] but is quantitatively poor at describing the metastable gas–liquid coexistence. Specifically it predicts a critical value of ϕ_p that is in reasonable agreement with simulation but a critical colloid volume fraction of $\phi_c \sim 0.57$ that is unphysically large [14].

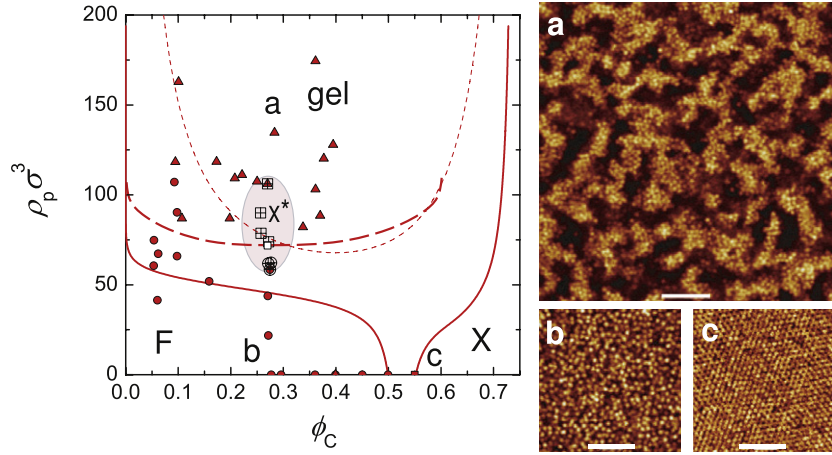


Figure 2. Phase diagram at room temperature in the colloid volume fraction ϕ_c and polymer reservoir number density ρ_p plane. Symbols are experimental data; circles are fluid (F), triangles are gels and squares are crystals (X). Shaded area marked X^* denotes samples which crystallized on the experimental timescale: hatched squares were initially gels, and hatched circles were initially fluids. The data are compared with theoretical predictions for the AO model, with $q = 0.214$, from free-volume theory for fluid–solid coexistence (solid lines) [13] and for the liquid–gas spinodal (short-dashed line) (equation (3)). The unfilled square is the AO critical point according to our B_2^{*AHS} criterion and the long dashed line is a sketch of the accompanying spinodal. (a)–(c) are confocal microscopy images taken at room temperature of a gel (a), fluid (b) and (hard sphere) crystal (c) at states in the phase diagram shown in the main panel. Bars = 20 μm .

In figure 2 we plot the fluid–fluid spinodal for $q = 0.214$, the value that corresponds to the experimental system at room temperature $T = 25^\circ\text{C}$, calculated from free-volume theory using the analytical expression derived by Schmidt *et al* [36]:

$$\phi_p = \frac{\theta_1^4 \theta_2 / \phi_c}{\alpha (12\theta_1^3 + 15q\theta_1^2\theta_2 + 6q^2\theta_1\theta_2^2 + q^3\theta_2^3)} \quad (3)$$

where $\theta_1 = (1 - \phi_c)$, $\theta_2 = (1 + 2\phi_c)$ and α is the free-volume fraction [13, 36].

One finds that the critical point is at about $\phi_c = 0.40$, $\phi_p = 0.35$. Once again the critical colloid fraction appears rather high. We shall argue that a more accurate value is $\phi_c \sim 0.27$.

Clearly a more reliable prescription is required to estimate the critical point and therefore the location of the binodal. For models like the present, where attractive interactions are short-ranged (sticky), Vliegthart and Lekkerkerker [37] and Noro and Frenkel [38] argued that a useful estimate of the critical temperature (or interaction strength) could be obtained by considering the reduced, with respect to HS, second virial coefficient given by

$$B_2^* = \frac{3}{\sigma^3} \int_0^\infty dr r^2 [1 - \exp(-\beta u(r))] \quad (4)$$

where $u(r)$ is the pair potential. These authors proposed that for a wide class of model fluids $B_2^* \sim -1.5$ at the critical temperature. Later Largo and Wilding [39] carried out simulations for effective (depletion) potentials calculated for additive binary HS systems with size ratios $q = 0.1$ and 0.05 . For these small ratios the effective pair potentials are similar to the AO potential equation (1), but with an additional repulsive barrier.

For all the potentials they considered, Largo and Wilding found that the value of B_2^* at criticality obtained from simulation was very close to $B_2^{*AHS} = -1.207$, i.e. the value

reported for the adhesive hard sphere (AHS) model at its critical point [40]. Ashton applied the same criterion for the AO potential with $q = 0.1$ [33]. He found that his simulation result for the critical polymer reservoir fraction ϕ_p was 0.249, very close to the value 0.248 given by the B_2^{*AHS} criterion. We also considered the simulation results of Fortini *et al* [25] for the AO model with $q = 0.15$. In this case the critical value of ϕ_p is ~ 0.316 which is again close to the value 0.313 from the B_2^{*AHS} criterion. Since the size ratios we consider are not vastly larger than those considered above, we chose to estimate the critical value of ϕ_p by calculating B_2^* for the AO potential equation (1) and employing the B_2^{*AHS} criterion. In order to estimate the gas–liquid critical colloid volume fraction we used the mapping to the square-well potential proposed by Noro and Frenkel [38] to obtain an effective range. For the three temperatures, i.e. the three q values, that we consider the estimate of the critical colloid fraction is about 0.27 which happens to be equal to the AHS value [40].

It is important to note that the simulations of the AO model, and of other models with short-ranged attraction, report broad, in ϕ_c , colloidal gas–liquid coexistence curves extending to large values of ϕ_c and it is clear that extracting an accurate value for the critical colloid fraction can be difficult. Our resulting estimates of the AO model gas–liquid critical points are shown as open squares in figures 2 and 4 where we also sketch putative spinodals. Since our estimates are based on empirical recipes we remark that using the slightly higher value of -1.174 for the critical value of B_2^{*AHS} , reported by Largo *et al* [41], makes no discernible difference in our plots. Note also that their revised value of the critical packing fraction for AHS is 0.29, only slightly bigger than the earlier result for AHS. Moreover were we to employ the original estimate for the critical value of B_2^* , namely -1.5 , we find this results in only minor changes (about 4%) to the critical value of ϕ_p , for the size ratios relevant for our systems.

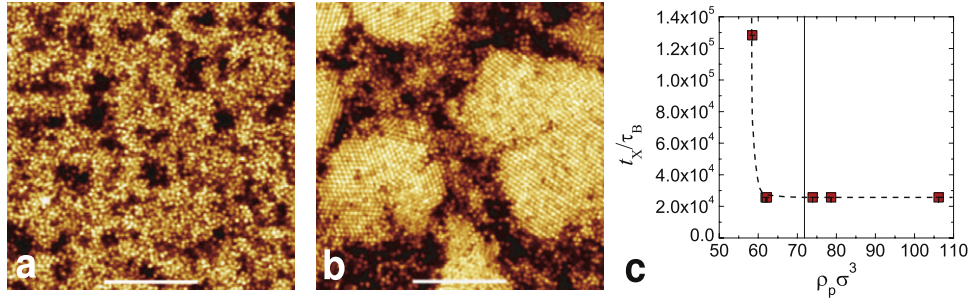


Figure 3. Crystallization in colloid–polymer mixtures at room temperature. Image (a) immediately after preparation, (b) after 1 day. Bars = 20 μm . (c) Crystallization times in units of the Brownian time τ_B as a function of polymer number density. Here samples have colloid volume fraction $\phi_c \approx 0.27$. Vertical line is the critical polymer number density estimated for the AO model, with $q = 0.214$, from the B_2^{*AHS} criterion. Dashed line is a guide to the eye.

3. Results

3.1. Room-temperature behaviour

We begin our presentation of results with the phase diagram at ambient conditions as shown in figure 2. Throughout we work in the colloid volume fraction ϕ_c and polymer reservoir number density ρ_p plane. We calculate ρ_p following the free-volume prescription for the AO model [13]: $\rho_p = \rho_p^{\text{exp}} / \alpha$, where ρ_p^{exp} is the experimental value for the polymer number density and α is the free-volume fraction entering equation (3). In the free-volume approximation, α depends on q and ϕ_c only [14]. For a size ratio $q \sim 0.2$ and colloid volume fractions up to $\phi_c \sim 0.4$ we expect this approximation to be accurate. Our choice of representation is motivated by two considerations: firstly, polymer number density is conserved during heating and cooling (while polymer ‘volume fraction’ emphatically is not), and secondly, the reservoir representation permits easy visual comparison with theoretical gas–liquid spinodal lines and critical points.

We calculate theoretical phase boundaries as outlined in section 2.2: fluid–solid coexistence is determined using free-volume theory [13] and the metastable gas–liquid critical point is estimated using the B_2^{*AHS} criterion. Experimentally, along the hard sphere line $\phi_p = 0$ (x -axis in figure 2) we find hard sphere crystallization for $\phi_c > 0.54$ as shown in figure 2(c). However, upon addition of polymer, we found fluid states around the AO fluid–solid phase boundary and gelation at higher polymer concentration. Only around the estimated AO gas–liquid critical point was a pocket of states found which crystallized on the experimental timescale of 6 days. This is the shaded region in figure 2.

We already remarked that the fluid–gelation boundary is often identified with the gas–liquid spinodal [26, 27]. In figure 2 we plot the spinodal calculated from free-volume theory, i.e. equation (3), and a sketch of where the spinodal should be located for the AO model, based on our B_2^{*AHS} criterion for the critical point. As mentioned earlier, free-volume theory grossly overestimates the colloid critical fraction for this size ratio $q = 0.214$ thus in making comparison with experiment it is appropriate to focus on the B_2^{*AHS} result. We observe that the states identified as gels (triangles) all lie within the (putative) AO spinodal.

Note that a typical confocal image of a gel is shown in figure 2(a). Below the estimated AO gas–liquid critical point we find only fluid states (circles) and a typical image of a fluid is shown in figure 2(b). We may conclude that the AO critical point provides an excellent indicator of the location of the experimentally observed transition between fluid and gel states at room temperature.

3.2. Critical enhancement of crystallization

Crystallization of colloid–polymer mixtures at room temperature is illustrated in figure 3. The crystals formed in the shaded region of figure 2 are markedly different from those formed in the absence of polymer (figure 2(c)) in that the system is at a much lower colloid packing fraction. We determined crystallization by visual inspection of images and define the crystallization time t_x as the time at which more than 50% of the images of the sample were predominantly crystals. In practice, we found that the vast majority of the sample was crystalline, figure 3(b) is a typical example. Crystallization times vary from 1 to 6 days. We observe crystallization only in a small ‘pocket’ around the critical polymer number density $\rho_p^c \sigma^3 \sim 72$, predicted by the AO model.

Some samples which crystallized were fluids prior to freezing (hatched circles in figure 2), while some were gels (hatched squares in figure 2). That crystallization is found to occur in the neighbourhood of the (metastable) colloidal gas–liquid critical point predicted by our B_2^{*AHS} criterion is remarkable and we explore this aspect further in figure 3(c) where we plot the crystallization time as a function of polymer density. We see there is a rapid variation of crystallization time. The unit of time employed is the Brownian time, defined as $\tau_B = \pi \eta \sigma^3 / k_B T$, where η is the viscosity, equal to 3.36 s for this system. For values of ρ_p inside the AO spinodal and slightly below the critical point, t_x is about $2.5 \times 10^4 \tau_B$. For smaller values in the (metastable) one-phase fluid region, moving further from criticality, the crystallization time increases rapidly and takes values outside the experimental time-window. This is consistent with the two-step nucleation scenario of ten Wolde and Frenkel [28].

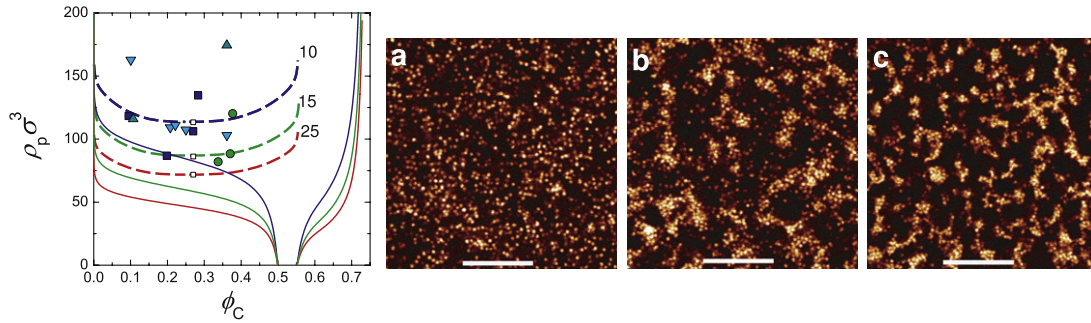


Figure 4. The fluid–gel transition at different temperatures. Images ((a)–(c)) show a typical experiment where the transition temperature is found by ‘quenching’ a colloid–polymer mixture by heating. Here $\phi_c = 0.107$ and $\rho_p = 116\sigma^{-3}$. (a) 8.5 °C, fluid, (b) 10.2 °C, condensing, (c) 11.8 °C, gel. The transition temperature is then identified as around 10 °C. In the main panel, experimental data indicate fluid–gel transitions at 10 °C (blue squares), 11 °C (turquoise up triangles), 12 °C (cyan down triangles) and 16 °C (green circles). As in figure 2, AO free-volume theory fluid–crystal coexistence lines are solid, critical points (unfilled squares) follow from our B_2^{*AHS} criterion and are shown with accompanying sketched spinodal (long dashed lines). These are plotted for room temperature (25 °C), 15 °C and 10 °C as indicated, corresponding to $q = 0.214, 0.197$ and 0.176 , respectively. Bars = 20 μm .

3.3. Response to temperature

We now consider the effect of temperature on our system. The results are given in figure 4. Using the temperature stage we cool the system to around 10 °C. The images in figures 4(a)–(c) show the effect of then gently heating the system. A metastable fluid (a) condenses (b) and finally forms a gel (c). The phase diagrams shown in the main panel pertain to the AO model and are obtained using the same prescriptions as in figure 2. It is assumed that the only effect of temperature T is to change the radius of gyration according to equation (2) and we calculate the size ratio using $q = 2R_G(T)/\sigma$. We find $q = 0.214, 0.197$ and 0.176 for $T = 25$ °C, 15 °C and 10 °C, respectively. Within the context of the free-volume approximation the fluid–solid coexistence lines in the ϕ_c – ϕ_p plane change little over this range of q and we fixed these to be the lines for $q = 0.18$. It is the scaling with $(\sigma/\sigma_p)^3$, from the polymer volume fraction to the polymer reservoir density, that gives rise to the variation of phase boundaries with temperature shown in the figure. Although the experimental data show considerable scatter, which we attribute predominantly to sedimentation effects, there is reasonable overall agreement with the theoretical predictions. Specifically we find that a transition from a fluid to a gel as illustrated in figures 4(a)–(c) occurs at temperatures broadly consistent with the location of the gas–liquid spinodals as predicted by our B_2^{*AHS} criterion. It appears that the assumption of ideal polymer behaviour is a reasonable first step to treating the temperature response of colloid–polymer mixtures.

Our particle-resolved images are ideal for understanding the local behaviour of spinodal decomposition. For example, inspection of figures 4(b) and (c) reveals the birth of droplets of colloidal liquid. Particularly striking is that we can immediately ascertain that the liquid droplets become denser with time as the temperature increases, in the sense that the colloids are closer together in figure 4(c) than in (b). This is consistent with the idea that, even in droplets of just a few tens of particles, the droplet density is similar (if not identical) to the bulk liquid spinodal density, and that, here quenching

deeper by increasing temperature leads to a denser colloidal liquid which eventually undergoes dynamical arrest.

4. Conclusions

We have examined the room-temperature behaviour of a colloid–polymer mixture and its response to temperature quenches. To the best of our knowledge, these are the first particle-resolved studies of the effects of temperature. At ambient conditions, the location of the fluid–gel transition is well described by an estimate of the colloidal gas–liquid spinodal based on a second virial coefficient criterion for the effective one-component Asakura–Oosawa model. Although free-volume theory provides a reasonable description of fluid–crystal coexistence, we emphasize that this approximation predicts a gas–liquid spinodal which lies at unphysically large colloid volume fractions.

The response to temperature is consistent with our assumptions that the polymers can be treated as ideal, and that the radius of gyration follows a simple fit to experimental results [31] (equation (2)). This opens the way to 3D particle-resolved studies of a variety of phenomena related to systems with attractive interactions which are tunable *in situ*.

We find crystallization on observable timescales close to the metastable gas–liquid critical point predicted by our B_2^{*AHS} criterion. Assuming the mapping we have carried out is accurate, we find crystallization in the (metastable) one-phase region below the critical point, on a timescale which increases at state points further from criticality, as well as in the (metastable) two-phase region. This contrasts with results from Brownian dynamics simulations where crystallization was found only in the metastable gas–liquid two-phase region [25, 42]. We attribute this to the very much longer timescale accessed in the experiments.

We comment on the apparent discrepancy between our results and those of Ilett *et al* [15], who found crystallization closer to the fluid–crystal boundary predicted by free-volume theory in a comparable system (with size ratio $q = 0.08$). Specifically, their samples crystallized in the region of the

phase diagram where the (one-phase) fluid is metastable with respect to gas–crystal coexistence. Except close to gas–liquid criticality and at high colloid volume fraction ($\phi_c > 0.54$), our samples did not crystallize. However in their case, the colloid diameter was $\sigma \approx 400$ nm, compared to $\sigma \approx 1080$ nm here. This has drastic consequences for the dynamics of the system, as the time for a colloid to freely diffuse over its own diameter scales with the cube of the particle size. Thus the effective timescales are around 20 times smaller in their work. Typical crystallization times were around 6 h in their case. This corresponds to 120 h for our systems, which is far beyond the experimental limits of around one hour imposed by sedimentation. Observations such as this underline the challenges for self-assembly in this size range and serve to emphasize the very strong dependence of timescales upon colloid size in these systems. Since, our approach is entirely reversible, it affords the possibility of implementing a colloidal analogue of annealing, which may well improve the quality of self-assembled colloidal crystals.

Finally we note that most computer simulations [25, 42] neglect hydrodynamic interactions (HI) between the colloids. These are believed to have a profound influence on structure in colloidal gels [43]. Since the rate of effective quenching leading to gel formation can be controlled, it is possible using our technique to explore the ‘instantaneous quench’ regime where colloid–colloid interactions are fixed as a function of time (and HI may be important) as well as the quasi-equilibrium slow ‘quench’ regime where particle diffusion dominates. In combination with simulation [42], our technique may provide a means to probe the effect of hydrodynamics on the structure of colloidal gels formed by arrested gas–liquid phase separation.

Acknowledgments

SLT and CPR acknowledge the Royal Society for financial support and EPSRC, grant code EP/H022333/1, for provision of the confocal microscope used in this work. Gregory N Smith is acknowledged for performing preliminary experiments. Daan Frenkel, Rob Jack and Richard Sear are thanked for many stimulating discussions.

References

- [1] Poon W C K 2002 The physics of a model colloid–polymer mixture *J. Phys.: Condens. Matter* **14** R859–80
- [2] Lekkerkerker H N W and Tuinier R 2011 *Colloids and the Depletion Interaction (Lecture Notes in Physics vol 833)* (Berlin: Springer)
- [3] Asakura S and Oosawa F 1954 On interaction between 2 bodies immersed in a solution of macromolecules *J. Chem. Phys.* **22** 1255–6
- [4] Asakura S and Oosawa F 1958 Interaction between particles suspended in solutions of macromolecules *J. Polym. Sci.* **33** 183–92
- [5] Long J A, Osmond D W and Vincent B 1972 The equilibrium aspects of weak flocculation *J. Colloid Interface Sci.* **42** 545–53
- [6] Vrij A 1976 Polymers at interfaces and interactions in colloidal dispersions *Pure Appl. Chem.* **48** 471–83
- [7] Pham K N et al 2002 Multiple glassy states in a simple model system *Science* **296** 104–6
- [8] de Hoog E H A, Kegel W K, van Blaaderen A and Lekkerkerker H N W 2001 Direct observation of crystallisation and aggregation in a phase-separating colloid–polymer suspension *Phys. Rev. E* **64** 021407
- [9] Aarts D G A L, Schmidt M and Lekkerkerker H N W 2004 Direct observation of thermal capillary waves *Science* **304** 847–50
- [10] Royall C P, Aarts D G A L and Tanaka H 2007 Bridging length scales in colloidal liquids and interfaces from near-critical divergence to single particles *Nature Phys.* **9** 636–40
- [11] Savage J R and Dinsmore A D 2009 Experimental evidence for two-step nucleation in colloids *Phys. Rev. Lett.* **102** 198302
- [12] Gast A P, Hall C K and Russel W B 1983 Polymer-induced phase separations in nonaqueous colloidal suspensions *J. Colloid Interface Sci.* **96** 251–67
- [13] Lekkerkerker H N W, Poon W C K, Pusey P N, Stroobants A and Warren P B 1992 Phase-behavior of colloid plus polymer mixtures *Europhys. Lett.* **20** 559–64
- [14] Dijkstra M, Brader J M and Evans R 1999 Phase behaviour and structure of model colloid–polymer mixtures *J. Phys.: Condens. Matter* **11** 10079–106
- [15] Ilett S M, Orrock A, Poon W C K and Pusey P N 1995 Phase behaviour of a model colloid–polymer mixture *Phys. Rev. E* **52** 1344–52
- [16] Dijkstra M, van Roij R and Evans R 2000 Effective interactions, structure, and isothermal compressibility of colloidal suspensions *J. Chem. Phys.* **113** 4799–807
- [17] Royall C P, Louis A A and Tanaka H 2007 Measuring colloidal interactions with confocal microscopy *J. Chem. Phys.* **127** 044507
- [18] de Gennes P G 1979 *Scaling Concepts in Polymer Physics* (Ithaca, NY: Cornell University Press)
- [19] Alsayed A M, Dogic Z and Yodh A G 2004 Melting of lamellar phases in temperature sensitive colloid–polymer suspensions *Phys. Rev. Lett.* **93** 057801
- [20] Hertlein C, Helden L, Gambassi A, Dietrich S and Bechinger C 2008 Direct measurement of critical Casimir forces *Nature* **451** 172–5
- [21] Guo H, Narayanan T, Sztuchi M, Schall P and Wegdam G H 2007 Reversible phase transition of colloids in a binary liquid solvent *Phys. Rev. Lett.* **100** 188303
- [22] Bonn D, Otwinowski J, Sacanna S, Guo H, Wegdam G and Schall P 2009 Direct observation of colloidal aggregation by critical Casimir forces *Phys. Rev. Lett.* **103** 156101
- [23] Elsner N, Snoswell D R E, Royall C P and Vincent B V 2009 Simple models for 2D tunable colloidal crystals in rotating AC electric fields *J. Chem. Phys.* **130** 154901
- [24] Ivlev A, Morfill G, Loewen H and Royall C P 2012 *Complex Plasmas and Colloidal Dispersions: Particle-Resolved Studies of Classical Liquids and Solids (Series in Soft Condensed Matter vol 5)* (Singapore: World Scientific)
- [25] Fortini A, Sanz E and Dijkstra M 2008 Crystallization and gelation in colloidal systems with short-ranged attractive interactions *Phys. Rev. E* **78** 041402
- [26] Verhaegh N A M, Asnaghi D, Lekkerkerker H N W, Giglio M and Cipelletti L 1997 Transient gelation by spinodal decomposition in colloid–polymer mixtures *Physica A* **242** 104–18
- [27] Lu P J, Zaccarelli E, Ciulla F, Schofield A B, Sciortino F and Weitz D A 2008 Gelation of particles with short-range attraction *Nature* **435** 499–504
- [28] ten Wolde P R and Frenkel D 1997 Enhancement of protein crystal nucleation by critical density fluctuations *Science* **277** 1975–8

- [29] Galkin O and Vekilov P 2000 Control of protein crystal nucleation around the metastable liquid–liquid phase boundary *Proc. Natl Acad. Sci. USA* **97** 6277–81
- [30] Vekilov P G 2010 Nucleation *Cryst. Growth Des.* **10** 5007–19
- [31] Berry G C 1966 Thermodynamic and conformational properties of polystyrene. I. Light-scattering studies on dilute solutions of linear polystyrenes *J. Chem. Phys.* **44** 4550–64
- [32] Vincent B 1990 The calculation of depletion layer thickness as a function of bulk polymer concentration *Colloids Surf.* **50** 241–9
- [33] Ashton D 2011 personal communication
- [34] Vink R L C and Horbach J 2004 Grand canonical Monte Carlo simulation of a model colloid polymer mixture: coexistence line, critical behavior, and interfacial tension *J. Chem. Phys.* **121** 3253–8
- [35] Lo Verso F, Vink R L C, Pini D and Reatto L 2006 Critical behavior in colloid–polymer mixtures: theory and simulation *Phys. Rev. E* **73** 061407
- [36] Schmidt M, Loewen H, Brader J M and Evans R 2002 Density functional theory for a model colloid–polymer mixture: bulk fluid phases *J. Phys.: Condens. Matter* **14** 9353–82
- [37] Vliegthart G A and Lekkerkerker H N W 2000 Predicting the gas–liquid critical point from the second virial coefficient *J. Chem. Phys.* **112** 5364–9
- [38] Noro M G and Frenkel D 2000 Extended corresponding-states behavior for particles with variable range attractions *J. Chem. Phys.* **113** 2941–4
- [39] Largo J and Wilding N B 2006 Influence of polydispersity on the critical parameters of an effective-potential model for asymmetric hard-sphere mixtures *Phys. Rev. E* **73** 036115
- [40] Miller M A and Frenkel D 2003 Competition of percolation and phase separation in a fluid of adhesive hard spheres *Phys. Rev. Lett.* **90** 135702
- [41] Largo J, Miller M A and Sciortino F 2008 The vanishing limit of the square-well fluid: the adhesive hard-sphere model as a reference system *J. Chem. Phys.* **128** 134513
- [42] Royall C P and Malins A 2012 The role of quench rate in colloidal gels *Faraday Discuss.* (arXiv:1203.0664v1 [cond-mat.soft])
- [43] Furukawa A and Tanaka H 2010 Key role of hydrodynamic interactions in colloidal gelation *Phys. Rev. Lett.* **104** 245702